VIP Therapeutic Nanoparticles

DOI: 10.1002/anie.201203780

Ceria Nanoparticles that can Protect against Ischemic Stroke**

Chi Kyung Kim, Taeho Kim, In-Young Choi, Min Soh, Dohoung Kim, Young-Ju Kim, Hyunduk Jang, Hye-Sung Yang, Jun Yup Kim, Hong-Kyun Park, Seung Pyo Park, Sangseung Park, Taekyung Yu, Byung-Woo Yoon, Seung-Hoon Lee, and Taeghwan Hyeon**

Ischemic stroke is the leading cause of adult disability in the United States and the second leading cause of death worldwide.[1] Reactive oxygen species (ROS), such as the superoxide anion ($O_2^{\bullet -}$), hydrogen peroxide (H_2O_2), and hydroxyl radical ($HO^{\bullet -}$), are generated and accumulate during ischemic periods. These species induce oxidative damage, which is one of the most critical mechanisms responsible for causing ischemic injury,[2] and oxidative damage elicits stroke-related cell death mechanisms, such as apoptosis.[3] As a result, neuronal networks and neurovascular units are completely destroyed, and the brain function is stopped. However, no effective neuroprotective therapy for ischemic stroke has been developed for clinical practice. Despite the availability of antioxidant drugs, no treatments have been proven to protect against oxidative damage after acute ischemic stroke in humans.

Ceria nanoparticles are known to exhibit free radical scavenging activity by reversibly binding oxygen and shifting between the Ce^{3+} (reduced) and Ce^{4+} (oxidized) forms at the particle surface.[4] From the crystal structure of ceria nanoparticles, cerium ions mostly exist in the valence state of Ce^{4+}; however, reduction in particle size results in oxygen vacancies from the particle surface, which allows the coexistence of Ce^{3+}.[5] Moreover, the catalytic properties of ceria nanoparticles can be further enhanced by using ultrasmall nanoparticles of less than 4 nm.[6] The ability of ceria nanoparticles to switch between oxidation states and scavenge free radicals is comparable to biological antioxidants. In fact, it was recently reported that ceria nanoparticles exhibit superoxide dismutase-mimetic activity[7,8] and catalase-mimetic activity[9,10] to protect cells against two dominant ROS, the superoxide anion and hydrogen peroxide. Herein, we report that ceria nanoparticles can protect against ischemic stroke in an in vivo animal model.

Ceria nanoparticles were prepared using a modified reverse micelle method,[11] which enabled the synthesis of uniformly sized ceria nanoparticles under facile and mild reaction conditions. Transmission electron microscope (TEM) images revealed discrete and uniform 3 nm-sized ceria nanoparticles (Figure 1 a). High-resolution TEM images revealed a cross-lattice pattern, demonstrating the highly crystalline nature of these particles, despite the low reaction temperature (Figure 1 b). The selected area electron diffraction (SAED) pattern (Figure 1 c) and X-ray diffraction (XRD) pattern (Figure 1 d) revealed a cubic fluorite structure (JCPDS card no. 34-0394). The particle size, estimated using the Scherrer formula, was 3.3 nm, which matched very well with that measured using TEM. In contrast to the white color of pure CeO_2, the prepared nanoparticles exhibited a yellowish color because they were composed of not only cerium(IV) oxide but also cerium(III) oxide.[12] X-ray photoelectron spectroscopy (XPS) analysis was used to identify the valence state of Ce^{3+} (peaks at 885.0 and 903.5 eV) and Ce^{4+} (peaks at 882.1, 888.1, 898.0, 900.9, 906.4, and 916.4 eV), confirming the mixed valence state (Figure 1 e).[7]

Good colloidal stability and narrow size distribution are essential for the successful biomedical application of ceria nanoparticles. Because of the strong hydrophobic nature of the synthesized ceria nanoparticles, we used the PEGylation method for stabilization, enabling the nanoparticles to circulate longer in the blood stream by reducing nonspecific binding and uptake by organs.[13,14] Briefly, nanoparticles were transferred to aqueous media by encapsulation with phospholipid–polyethylene glycol (PEG; Figure 1 g).[15] The nanoparticles showed excellent colloidal stability without agglomerations in phosphate-buffered saline (PBS) as well as in blood plasma, and their hydrodynamic diameters were maintained at 18–30 nm for over 10 days (Figure 1 f). The ROS-scavenging activity of the ceria nanoparticles, assessed by the superoxide dismutase-mimetic assay and catalase-mimetic assay, was found to be dose-dependent (Supporting Information, Figure S2). Furthermore, we examined the autocatalytic properties of ceria nanoparticles using visual inspection of color change and UV/Vis spectroscopic analysis.[16,17] When H_2O_2 solutions of various concentrations were added to PBS solutions containing 5 mM ceria nanoparticles,

[*] Dr. C. K. Kim,[+] I.-Y. Choi, Dr. D. Kim, Y.-J. Kim, Dr. H. Jang, H.-S. Yang, Dr. J. Y. Kim, Dr. H.-K. Park, Prof. B.-W. Yoon, Prof. S.-H. Lee
Department of Neurology, Seoul National University Hospital, and Department of Neurology, College of Medicine and Neuroscience Research Institute, Medical Research Center, Seoul National University
Seoul 110-744 (Korea)
E-mail: sb0516@snu.ac.kr
T. Kim,[+] M. Soh, Dr. S. P. Park, S. Park, Dr. T. Yu, Prof. T. Hyeon
Center for Nanoparticle Research, Institute for Basic Science (IBS), and School of Chemical and Biological Engineering, Seoul National University
Seoul 151-742 (Korea)
E-mail: thyeon@snu.ac.kr
[+] These authors contributed equally to this work.

[**] This work was supported by a grant of the Korean Health Technology R&D Project, Korean Ministry of Health & Welfare (A111014).

Supporting information for this article is available on the WWW under http://dx.doi.org/10.1002/anie.201203780.

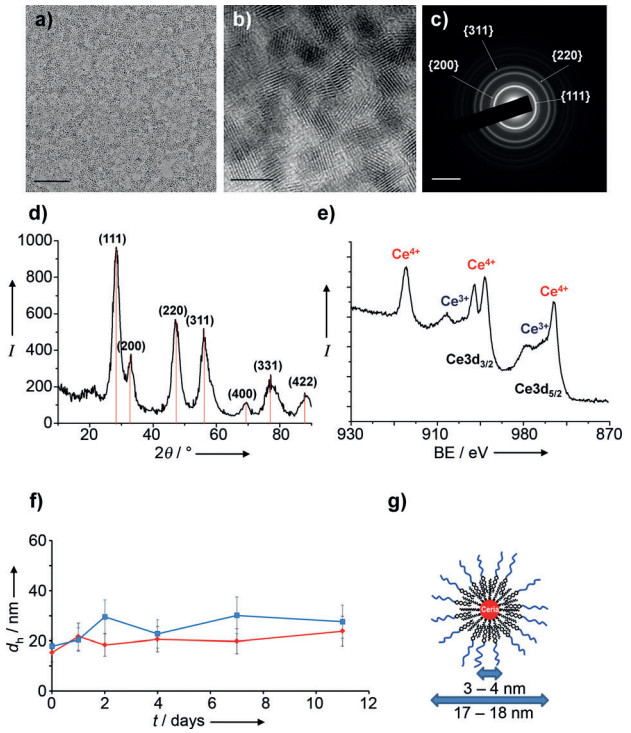

Figure 1. Characterization of ceria nanoparticles. a) TEM images reveal discrete and uniform 3 nm-sized ceria nanoparticles. Scale bar = 100 nm. b) High-resolution TEM images reveal a cross-lattice pattern, demonstrating the highly crystalline nature of the ceria nanoparticles. Scale bar = 5 nm. c, d) The SAED pattern and XRD pattern reveal a cubic fluorite structure. Scale bar = 5 nm^{-1}. e) XPS analysis to identify the valence state of cerium ions and confirm corresponding binding energy (BE) peaks for Ce^{3+} (885.0 and 903.5 eV) and Ce^{4+} (882.1, 888.1, 898.0, 900.9, 906.4, and 916.4 eV). f) Hydrodynamic diameters d_h from dynamic light scattering of phospholipid-PEG-capped ceria nanoparticles (4.5 mM) in PBS (◆, red) and blood plasma (■, blue), showing that they do not agglomerate and are very well dispersed for more than ten days in the physiological medium. g) The ceria nanoparticle geometry after hydrophilic encapsulation with phospholipid-PEG (core diameter d_c = 3–4 nm; hydrodynamic diameter d_h = 17–18 nm).

reversible autocatalytic activity persisted even after 3 weeks (Supporting Information, Figure S3).

To investigate the effects of ceria nanoparticles on ROS-induced cell death in vitro, CHO-K1 cells were incubated with *tert*-butyl hydroperoxide (tBHP), which increases intracellular ROS.[18] Using 3-(4,5-dimethylthiazol-2-yl)-2,5-diphenyltetrazolium bromide (MTT) assay, we found that 1 mM tBHP significantly increased cell death compared with the control (83%, $p < 0.05$; Supporting Information, Figure S4), while the addition of 0.125 mM ceria nanoparticles significantly increased cell viability (113%, $p < 0.05$). We also found that ceria nanoparticles were mostly detected in intracellular spaces, as shown by fluorescence imaging with rhodamine dye (Supporting Information, Figure S5). To investigate the concentration- and time-dependent cellular uptake, we performed fluorescence-activated cell sorting study using fluorescent dye-conjugated 3 nm-sized ceria nanoparticles (Supporting Information, Figure S6). The cellular uptake increased in a dose-dependent manner, and was saturated above 0.125 mM. The cellular uptake increased in a time-dependent manner. Taken together, our results demonstrate that ceria nanoparticles introduced into cells show protective effects against ROS-induced cell death in vitro, and this correlates with the results of a previous report.[19]

To investigate the neuroprotective effects of ceria nanoparticles in vivo, we induced ischemic stroke in rats and subsequently introduced ceria nanoparticles by intravenous injection. We then compared brain infarct volumes in rats treated with various doses of ceria nanoparticles to determine an optimal dose (Figure 2a,b). Low-dose ceria nanoparticles (0.1 and 0.3 mg kg^{-1}) did not decrease infarct volumes, whereas ceria nanoparticles at concentrations of 0.5 and 0.7 mg kg^{-1} considerably reduced infarct volumes up to 50% of those of the control group ($p < 0.05$). However, higher doses of ceria nanoparticles (1.0 and 1.5 mg kg^{-1}) failed to show a protective effect against stroke. To support these findings, we performed microscopic analysis of cell death in frozen brain sections using terminal deoxynucleotidyl transferase-mediated dUTP-biotin nick end labeling (TUNEL) assays (Figure 2c). Quantitative analysis showed that the number of TUNEL-positive cells was markedly decreased in the ceria-injected group (0.5 mg kg^{-1}; $p < 0.05$; Figure 2d). Collectively, we concluded that the optimal dose of ceria nanoparticles (0.5 to 0.7 mg kg^{-1}) had powerful neuroprotective effects in this rodent stroke model, and all subsequent experiments were performed using 0.5 mg kg^{-1} ceria nanoparticles. On the basis of the observed therapeutic window for ceria nanoparticles in vivo, we found that the indiscriminate use of nanoparticles without considering the optimal dose may not be protective and may even be harmful.[20,21] Recent studies using a hippocampal brain slice model[22] and spinal cord injury model[23] have shown that ceria nanoparticles may be protective against ischemic or traumatic neuronal damage in vitro. Thus, in the current study, we demonstrated this protective effect, using the optimal dose, in a living animal model of ischemic stroke to mimic human clinical settings.

As the brain is secured by the blood–brain barrier and ceria nanoparticles were injected intravenously in this study, we also analyzed the delivery of ceria nanoparticles through an in vivo study to determine whether intravenous injection could effectively localize ceria nanoparticles to the ischemic brain. For this experiment, concentrations of ceria nanoparticles were measured in various internal organs of rats using inductively coupled plasma–mass spectrometry analysis. Interestingly, while the concentration of ceria nanoparticles in the nonischemic brain was very low, the level of ceria nanoparticles increased strikingly 24 h after ischemia ($p < 0.05$; Figure 3a), exceeding the concentrations of nanoparticles observed in the kidneys and heart. The concentration of ceria nanoparticles in brain after stroke was increased in a dose-dependent manner with 0.5, 1.0, and 1.5 mg kg^{-1}. Next, we sought to track ceria nanoparticles microscopically using rhodamine B isothiocyanate-conjugated ceria nanoparticles and fluorescence microscopy analysis. As shown in Figure 3b, a significant number of positively stained cells were identified in the ischemic hemisphere, but very few cells were located in the nonischemic hemisphere. We conducted computerized visual augmentation using three-dimensional reconstruction

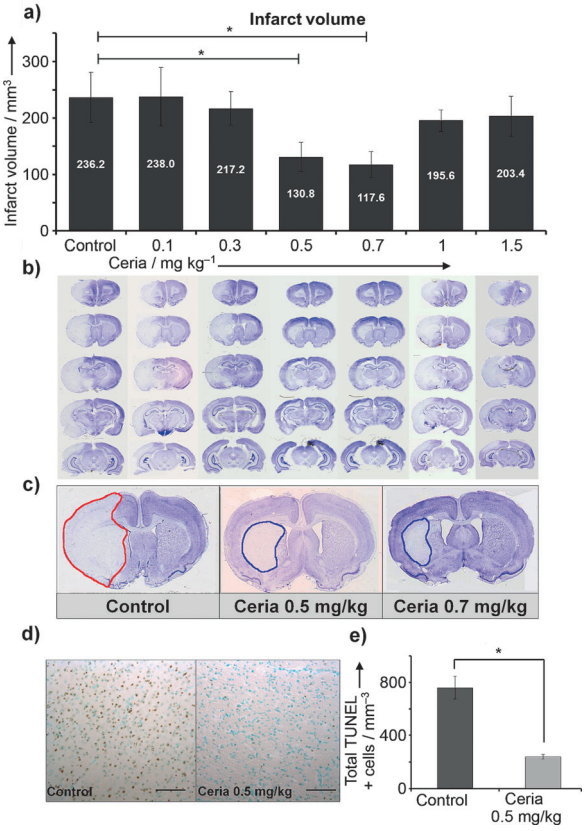

Figure 2. Infarct volume and ischemic cell death in vivo. a) Low-dose ceria nanoparticles (0.1 and 0.3 mg kg^{-1}) do not decrease infarct volumes, whereas 0.5 and 0.7 mg kg^{-1} ceria nanoparticles considerably reduce infarct volumes, to as little as 50% of those of the control group (*, $p < 0.05$). Higher doses of ceria nanoparticles (1.0 and 1.5 mg kg^{-1}) do not exhibit protective effects against stroke ($n = 12$ for each group, except 0.1 and 1.5 mg kg^{-1}, where $n = 6$). b) Brain slices from anterior (top) to posterior (bottom), with intervals of 2 mm. On Nissl-stained brains, infarcts are shown as pale blue-colored lesions, while undamaged region are stained as deep blue. Infarct areas were maximally decreased at 0.5 and 0.7 mg kg^{-1} ceria nanoparticles. c) Representative slices, clearly showing that 0.5 and 0.7 mg kg^{-1} ceria nanoparticles can significantly reduce infarct volumes. d) Microscopic analysis of cell death in brain slices using TUNEL. TUNEL-positive cells are shown in brown, and TUNEL-negative cells, which were counter-stained with methyl green, are shown in blue. The number of TUNEL-positive cells was reduced in the ceria-injected group (0.5 mg kg^{-1}). Scale bar = 100 μm. e) In our quantitative analysis, the number of TUNEL-positive cells decrease markedly in the ceria-injected group (*, $p < 0.05$; $n = 4$ each).

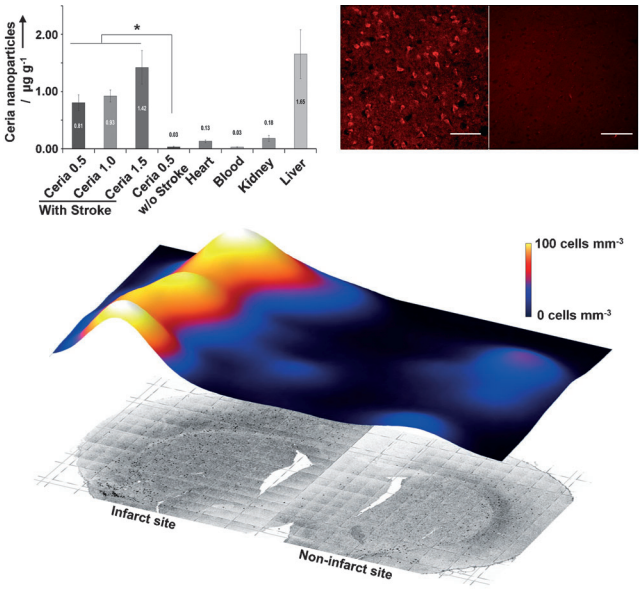

Figure 3. Biodistribution of ceria nanoparticles. a) The concentration of ceria nanoparticles in the nonischemic brain is very low, but significantly increases at 24 h after ischemia (*, $p < 0.05$); values were even higher than those observed in the kidneys and heart ($n = 8$ for brain with stroke, otherwise $n = 4$ each). b) Cells that were positively stained with rhodamine B isothiocyanate-conjugated ceria nanoparticles were identified to a great extent in the ischemic hemisphere (left), but only minimally in the nonischemic hemisphere (right). Scale bar = 100 μm. c) By using computerized visual augmentation with 3-dimensional reconstruction of fluorescence signals, signals for ceria nanoparticles greatly increase in the peri-infarct area in the ischemic hemisphere.

of the fluorescence signals, and found that the signals for ceria nanoparticles were significantly increased in the peri-infarct area in the ischemic hemisphere (Figure 3c). Thus, we demonstrated that intravenously injected ceria nanoparticles did not sufficiently permeate the normal brain tissue[24] but were able to permeate ischemic brain tissue; This was likely possible because brain ischemia leads to extensive breakage of the blood–brain barrier, which may facilitate passage of ceria nanoparticles into the brain.[25] Furthermore, the accumulation of ceria nanoparticles increased owing to their uniformity, small size, and prolonged blood circulation owing to PEGylation.

We investigated whether ceria nanoparticles reduce ROS and apoptosis in vivo because oxidative damage is a major cause of ischemic brain injury and elicits apoptotic cell death.[2,3] After a stroke, oxidized hydroethidine signals (as a measure of ROS) were lower in the ceria-injected group than in the control group ($p < 0.05$; Figure 4a,b), indicating that ceria nanoparticles acted as antioxidants after ischemia. To analyze ROS quantitatively, we performed the assay for lipid peroxides. The average concentration of lipid peroxides in stroke area was measured to be 24.6 ± 7.9 μM. After treating with 0.5 mg kg^{-1} of ceria nanoparticles, the concentration was significantly decreased to 15.5 ± 4.9 μM ($p < 0.05$; Figure 4c). To investigate the effects of ceria nanoparticles on apoptosis after stroke, we analyzed apoptotic TUNEL-positive cells (a subgroup of TUNEL-positive cells according to morphological criteria; Supporting Information, Figure S13). The number of apoptotic cells in the ceria nanoparticle-injected group was lower than that in the control group ($p < 0.05$; Figure 4d), and pro-apoptotic proteins, such as phospho-p53, cleaved caspase-3, and gelsolin, decreased in the ceria nanoparticle-injected group ($p < 0.05$; Figure 4e,f). ROS production and apoptosis are closely related because they both occur in the mitochondria. Furthermore, ROS directly stimulates apoptosis-regulated proteins, such as p53.[26,27] Recently, amine-modified single-walled carbon nanotubes were investigated as potential therapeutic agents

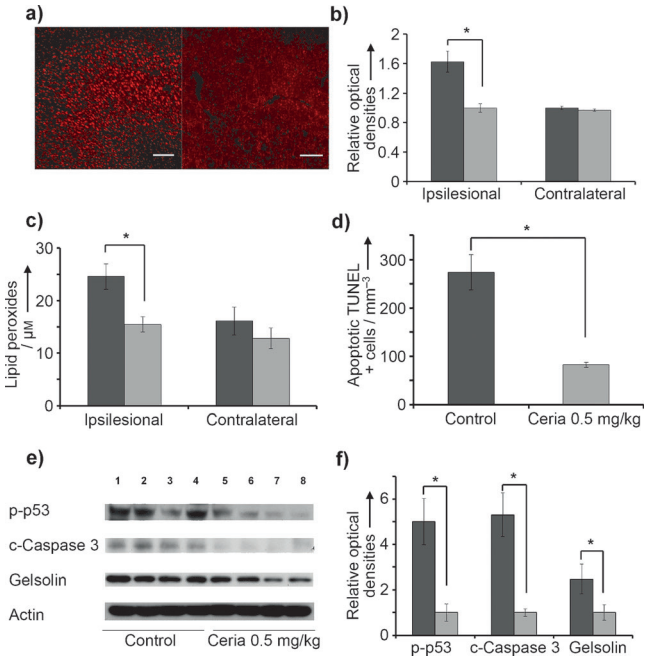

Figure 4. Scavenging of reactive oxygen species (ROS) and apoptosis-reducing effects. a) Oxidized hydroethidine signals (as a detector of ROS) decrease in the ceria nanoparticle-injected group (right) compared with the control group (left). b) Density of oxidized hydroethidine for the control (dark gray) and 0.5 mg kg^{-1} ceria (light gray). (*, $p<0.05$; $n=4$ each). Scale bar = 200 µm. c) Lipid peroxides in the stroke area decrease in the ceria-injected group compared with the control (*, $p<0.05$; $n=8$ each). d) Apoptotic terminal deoxynucleotidyl transferase-mediated dUTP-biotin nick end labeling (TUNEL)-positive cells (a subgroup of TUNEL-positive cells according to the morphologic criteria; see the Supporting Information) were analyzed. The number of apoptotic cells in the ceria-nanoparticle-injected group is lower than that in the control group (*, $p<0.05$; $n=4$ each). e), f) In western blotting analyses, pro-apoptotic proteins, such as phospho-p53, cleave caspase-3, and gelsolin decreases in the ceria nanoparticle-injected group compared with the control group (*, $p<0.05$; $n=4$ each). These proteins were obtained from cell extracts in the infarcted hemisphere.

for ischemic stroke through reducing apoptosis.[28] In a previous in vitro study, ceria nanoparticles decreased apoptosis as well as ROS.[29] Thus, the results of our current in vivo model support these previous studies, demonstrating that ceria nanoparticles can reduce apoptotic cell death by decreasing ROS, which may lead to a decreased infarct volume.

In conclusion, optimal doses of ceria nanoparticles (0.5 and 0.7 mg kg^{-1}) reduced ischemic brain damage. Our ceria nanoparticles targeted the damaged area by disruption of the blood–brain barrier after ischemia. Innovative nanotechnology such as the ceria nanoparticles studies presented here makes it possible to produce more chemically potent and biologically compatible materials. Previous studies evaluated the in vivo protective effects of ceria nanoparticles in only a few diseases, including retinal degeneration and cardiomyopathy.[30,31] This report is the first demonstration of the protective effects of ceria nanoparticles against ischemic stroke in living animals, offering hope and an alternative treatment modality for patients with ischemic stroke.

Received: May 16, 2012
Revised: July 30, 2012
Published online: September 11, 2012

Keywords: apoptosis · ceria nanoparticles · ischemic stroke · reactive oxygen species · therapeutic agents

[1] V. L. Roger, et al., *Circulation* **2012**, *125*, e20.
[2] C. L. Allen, U. Bayraktutan, *Int. J. Stroke* **2009**, *4*, 461.
[3] P. H. Chan, *J. Cereb. Blood Flow Metab.* **2001**, *21*, 2.
[4] I. Celardo, J. Z. Pedersen, E. Traversa, L. Ghibelli, *Nanoscale* **2011**, *3*, 1411.
[5] D. Sameer, P. Swanand, V. N. T. K. Satyanarayana, S. Seal, *Apply. Phys. Lett.* **2005**, *87*, 133113.
[6] W. J. Stark, *Angew. Chem.* **2011**, *123*, 1276; *Angew. Chem. Int. Ed.* **2011**, *50*, 1242.
[7] E. G. Heckert, A. S. Karakoti, S. Seal, W. T. Self, *Biomaterials* **2008**, *29*, 2705.
[8] C. Korsvik, S. Patil, S. Seal, W. T. Self, *Chem. Commun.* **2007**, 1056.
[9] T. Pirmohamed, J. M. Dowding, S. Singh, B. Wasserman, E. Heckert, A. S. Karakoti, J. E. S. King, S. Seal, W. T. Self, *Chem. Commun.* **2010**, *46*, 2736.
[10] S. Singh, T. Dosani, A. S. Karakoti, A. Kumar, S. Seal, W. T. Self, *Biomaterials* **2011**, *32*, 6745.
[11] T. Yu, J. Moon, J. Park, Y. I. Park, H. B. Na, B. H. Kim, I. C. Song, W. K. Moon, T. Hyeon, *Chem. Mater.* **2009**, *21*, 2272.
[12] H. Gu, M. D. Soucek, *Chem. Mater.* **2007**, *19*, 1103.
[13] A. S. Karakoti, S. Das, S. Thevuthasan, S. Seal, *Angew. Chem.* **2011**, *123*, 2024; *Angew. Chem. Int. Ed.* **2011**, *50*, 1980.
[14] P. Rivera-gil, D. J. D. Aberasturi, V. Wulf, B. Pelaz, P. D. Pino, Y. Zhao, J. M. D. L. Fuente, I. R. D. Larramendi, T. Rojo, X.-J. Liang, W. J. Parak, *Acc. Chem. Res.* **2012**, DOI: 10.1021/ar300039j.
[15] B. Dubertret, P. Skourides, D. J. Norris, V. Noireaux, A. H. Brivanlou, A. Libchaber, *Science* **2002**, *298*, 1759.
[16] J. M. Perez, A. Asati, S. Nath, C. Kaittanis, *Small* **2008**, *4*, 552.
[17] A. S. Karakoti, S. Singh, A. Kumar, M. Malinska, S. V. N. T. Kuchibhatla, K. Wozniak, W. T. Self, S. Seal, *J. Am. Chem. Soc.* **2009**, *131*, 14144.
[18] K. Zhao, G.-M. Zhao, D. Wu, Y. Soong, A. V. Birk, P. W. Schiller, H. H. Szeto, *J. Biol. Chem.* **2004**, *279*, 34682.
[19] A. S. Karakoti, S. Singh, J. M. Dowding, S. Seal, W. T. Self, *Chem. Soc. Rev.* **2010**, *39*, 4422.
[20] N. Singh, C. A. Cohen, B. A. Rzigalinski, *Ann. N. Y. Acad. Sci.* **2007**, *1122*, 219.
[21] M. Horie, K. Nishio, H. Kato, K. Fujuta, S. Endoh, A. Nakamura, A. Miyauchi, S. Kinugasa, K. Yamamoto, E. Niki, Y. Yoshida, Y. Hagihara, H. Iwahashi, *J. Biochem.* **2011**, *150*, 461.
[22] A. Y. Estevez, S. Pritchard, K. Harper, J. W. Aston, A. Lynch, J. J. Lucky, J. S. Ludington, P. Chatani, W. P. Mosenthal, J. C. Leiter, S. Andreescu, J. S. Erlichman, *Free. Radic. Biol. Med.* **2011**, *51*, 1155.
[23] M. Das, S. Patil, N. Bhargava, J.-F. Kang, L. M. Riedel, S. Seal, J. J. Hickman, *Biomaterials* **2007**, *28*, 1918.
[24] S. S. Hardas, D. A. Butterfield, R. Sultana, M. T. Tseng, M. Dan, R. L. Florence, J. M. Unrine, U. M. Graham, P. Wu, E. A. Grulke, R. A. Yokel, *Toxicol. Sci.* **2010**, *116*, 562.
[25] Y. Yang, G. A. Rosenberg, *Stroke* **2011**, *42*, 3323.
[26] K. Niizuma, H. Endo, P. H. Chan, *J. Neurochem.* **2009**, *109-(Suppl. 1)*, 133.

[27] K. Niizuma, H. Yoshioka, H. Chen, G. S. Kim, J. E. Jung, M. Katsu, N. Okami, P. H. Chan, *Biochim. Biophys. Acta Mol. Basis Dis.* **2010**, *1802*, 92.
[28] H. J. Lee, J. Park, O. J. Yoon, H. W. Kim, D. Y. Lee, D. H. Kim, W. B. Lee, N.-E. Lee, J. V. Bonventre, S. S. Kim, *Nat. Nanotechnol.* **2011**, *6*, 121.
[29] A. Clark, A. Zhu, K. Sun, H. R. Petty, *J. Nanopart. Res.* **2011**, *13*, 5547.
[30] J. Chen, S. Patil, S. Seal, J. F. McGinnis, *Nat. Nanotechnol.* **2006**, *1*, 142.
[31] J. Niu, A. Azfer, L. M. Rogers, X. Wang, P. E. Kolattukudy, *Cardiovasc. Res.* **2007**, *73*, 549.

